Physica A 508 (2018) 313–323

Contents lists available at ScienceDirect

Physica A

journal homepage: www.elsevier.com/locate/physa

A cascading failure model based on AC optimal power flow: Case study

Jian Li [a,b,c], Congling Shi [a,*], Changkun Chen [b], Leonardo Dueñas-Osorio [c]

[a] Beijing Key Laboratory of Metro Fire and Passenger Transportation Safety, China Academy of Safety Science and Technology, Beijing 100012, PR China
[b] Institute of Disaster Prevention Science and Safety Technology, Central South University, Changsha, Hunan 410075, PR China
[c] Department of Civil and Environmental Engineering, Rice University, Houston, TX 77005, USA

HIGHLIGHTS

- AC-based cascading failure model (ACCF model) is applied to IEEE power grids.
- The ACCF model is proved feasible.
- Some failed lines are not close to initial faulty elements in cascading failure.
- Loss curves are symmetric when branch failure rates are low and high respectively.

ARTICLE INFO

Article history:
Received 8 October 2017
Received in revised form 8 March 2018
Available online 16 May 2018

Keywords:
AC-based cascading failure model
Case study
Nodes failure
Branches failure

ABSTRACT

Simulating the grids cascading failure process is an essential means of preventing cascading failures. In traditional cascading failure models, DC power flow models are applied widely, but reactive power characteristic cannot be reflected. This study improves and applies an AC-based Cascading Failure model (called ACCF model), which captures bus load shedding and branch failures, all via AC power flow and optimal power flow analyses. Taking the IEEE 30- and 118-bus power systems as case studies, the ACCF model is proved feasible. With case studies, this study reveals that during the cascading failure, the broken branches are not necessarily close to the initial faulty elements, and some of the affected nodes/branches are "far" away from the initial faulty nodes. And as the initial branch failure probability increases, the system real power loss probability function gradually changes from approximate power distribution to a normal distribution. Meanwhile, the study also discovers that as the initial branch failure probability further increases, the system real power loss changes from a normal distribution to a distribution that appearing to be symmetric with the loss function under a low initial branch failure probability. The findings could facilitate grids safety and stable operation, as well as grids disaster prevention and relief.

1. Introduction

With the constant improvement of modernization level and the persistent advancement of intelligent power grids construction, large-scale electric power system interconnection has become an inexorable trend in countries around the world. However, interconnection of power grids is likely to result the power grids dynamic behavior become more

* Corresponding author.
E-mail addresses: lijianaky@chinasafety.ac.cn (J. Li), shicl@chinasafety.ac.cn (C. Shi), cckchen@csu.edu.cn (C. Chen), leonardo.duenas-osorio@rice.edu (L. Dueñas-Osorio).

https://doi.org/10.1016/j.physa.2018.05.081
0378-4371/

complicated, make it more sensitive to the load characteristics and make the issue of steady state more severe. All these characteristics along with the even bigger network resulted from power grids interconnection make it more susceptible to electric power catastrophe caused by cascading failures. The major power failures occurred in recent years also makes people more deeply recognize the necessity and urgency of preventing power grids cascading failure and damages caused thereby [1–3].

Building a cascading failure model is an important method for having an in-depth comprehension of grids operation pattern, preventing cascading failures, minimizing cascading failure range and damage and ensuring infrastructure system safety. At present, there are two types of models simulating grids cascading failures: complex network-based cascading failure models [4–6] and approximate dynamic behavior-based cascading failure models [7].

Complex network-based cascading failure models mainly include betweenness-based model [8], M-L model [9,10], dynamical redistribution model [11,12], cluster distribution model [13,14], CASCADE model, Branching process model [15], HOT (Highly Optimized Tolerance) model [16,17], etc. Complex network-based cascading failure model has such advantages as easy solution, few parameter inputs, high-efficiency, etc. However, these algorithms generally give large-extent approximate treatment and assumptions of the power grids. For example, betweenness-based model would assume that electric energy flow between any two nodes via the shortest path. M-L algorithm also has similar assumptions, and the model utilizes the total number of the shortest paths that passing through the node to define the node load. However the above assumptions usually have certain differences from actual power grids, thus, errors are inevitable with complex network-based cascading failure model, and as a result it is not easy to apply them to physical power grids.

Relatively speaking, approximate dynamic behavior-based cascading failure models simulate actual grids operation process as far as possible, of which the widely applied models mainly include OPA model [18], hidden failure model [19], (DC) optimal power flow cascading failure model, Manchester model [20–22], etc. An innovation of OPA model is that it divides the cascading failure development process into slow dynamic process and quick dynamic process, of which the slow dynamic process forecasts the load increase and system reliability improvement, etc. Starting with one power flow solution, the quick dynamic process utilizes Monte Carlo method to generate an initial failure on a random basis, and once there is a branch break, it would optimize the power flow distribution based on the DC power flow model. An advantage of this model is that it considers both slow dynamic and quick dynamic processes, which is more agreeable with the reality. Similar to OPA model, hidden model also uses Monte Carlo method to simulate initial failure of the line, and uses DC flow model to simulate the interlocked tripping process triggered off by covert fault under protection. Though these DC-based models are used widely, they also have come certain deficiencies. For example, reactive power characteristics cannot be reflected by DC-based models. Manchester model utilizes AC model to avoid the demerits of DC flow models. The model utilizes AC flow model and gives a comprehensive consideration to the various factors relevant to cascading failure development, including cascade and sympathetic tripping of transmission branches, heuristic representation of generator instability, under-frequency load shedding, post-contingency re-dispatch of active and reactive resources, and emergency load shedding to prevent a complete system blackout caused by a voltage collapse. However, the power flow solution process of Manchester model has not considered the economic dispatch of operation, and neither given a full consideration to the regulating function of the generator.

In order to simulate cascading failure occurring process more objectively, the authors have introduced an OPF (Optimal Power Flow) model to improve the AC flow model in Manchester model contained in Ref [23], and have built an ACCF (AC-based Cascading Failure) model. The ACCF model can give a reasonable consideration to economic dispatch, and the result achieved is more aligned with the actual grids operation norm.

On the basis of the ACCF model [23], here the authors introduce a constrained non-linear optimization method to help solving the ACOPF problem. Then the ACCF model is applied to the power grids by taking IEEE 30 and 118-bus systems as examples, in order to investigate the power grids cascading failure characteristics. Grids cascading failure characteristics as well as power loss distribution characteristics are studied under different failure quantities and failure probabilities of nodes and branches in the grid. In this manuscript, a node here denotes a substation or power station, and a branch denotes the electric line between two nodes. Research results of this paper can provide a basis for prevention of grids cascading failures and disaster prevention and reduction management of the power grids.

2. AC-based cascading failure model

The main process of ACCF model is as such: firstly, assume some of the nodes in the system are failed according to a certain principle; remove the failed nodes out of the system; determine new system status based on AC power flow and optimal power flow calculation results, and cut off part of the load when necessary; meanwhile, according to the power flow calculation result, if a steady state cannot still not be reached by cutting off part of the load, the model will then break the overload branch, and then recalculate the power flow distribution. Repeat the foregoing process, until the system reaches a new balance or the system splits into a number of isolated islands while a new balance is maintained within each island, finally evaluate the load loss resulted from the cascading failure. A basic introduction of this model is given below:

2.1. Basic assumptions

Basic assumptions of ACCF model are as follows:

(1) The status of a branch is binary: up (functional) or down (failed). Most of the current cascading failure models adopt this assumption.

(2) Artificial repair is not considered in the process of grids cascading failure.

(3) Initial grids failures are mutually independent.

(4) Node failure and offline will also cause the branch connected with it to be offline.

The power grids is replaced by a directed network having N nodes and K branches. One node represents one power generation station or substation, as have indicated above. These nodes include four categories: (i) Being both power supply and load; (ii) Being only power supply but not load; (iii) Being only load but not power supply; (iv) Being neither power supply nor load, but only a voltage transformation node. In our study, the first two categories are called power supply nodes on a unified basis, namely, power supply nodes; the last two are called substation nodes.

If node i is a power supply node, then the power supply meets $0 \leq P_i^{\min} \leq P_i^{\max}$ and $0 \leq Q_i^{\min} \leq Q_i^{\max}$, where $P_i^{\min}$ and $P_i^{\max}$ are respectively the minimum and maximum real power of power supply i, and $Q_i^{\min}$ and $Q_i^{\max}$ are respectively the minimum and maximum reactive power of the power supply i. If the power generator is in running state, its power output is bounded to be respectively between $P_i^{\min}$ and $P_i^{\max}$ and between $Q_i^{\min}$ and $Q_i^{\max}$. Of course, if the power generator is not working, the power output is 0.

If node i has any power load need (but unnecessarily a substation node, because a power supply may also have power load needs), then when load shedding has not occurred, the load is D_i. If any load shedding has occurred, then its actual load satisfies $[0, D_i)$.

2.2. AC-based cascading failure model

ACCF model first identifies the isolated island formed by the grids after initial failure. Then it simulates the cascading failure of the isolated grids until all island cascading failures stop, when the algorithm comes to an end. For each island, the following simulation is carried out:

S1. Check to see if this island has any power supply node.

S2. If there is no power supply node, then undoubtedly the grids within the said island will stop running, and all loads will not be satisfied.

S3. If there exists any power supply node, then the grids within the said island might be running, and a certain load needs may also be satisfied. Under this circumstance, the model will check if there exists any other nodes besides the said power supply node.

S4. If no other node exists, in other words, there exists only one power generation node, then the electric power load of that node is the maximum power of the generator or the actual power need, whichever is smaller, i.e. $\min(S_i, D_i)$.

S5. If there is still any other nodes, then it is necessary to conduct a power flow analysis of the island. Before power flow analysis, it is necessary to select a reference node. In ACCF model, the reference node is assigned as a power supply node randomly. The main purpose for selecting a reference node is to make sure that the Jacobian Matrix is a non-singular matrix.

S6. An ACOPF (Alternating Current Optimal Power Flow, ACOPF) analysis is conducted of the said island. Mathematically, the optimal power flow is a constrained non-linear optimization problem. Taken reference of [24], we utilize the following objective function and constraint conditions:

$$\min_x f(x) \tag{1}$$

$$g(x) = 0 \tag{2}$$

$$h(x) \leq 0 \tag{3}$$

$$x_{\min} \leq x \leq x_{\max} \tag{4}$$

Eq. (1) is the objective function, and Eqs. (2) to (4) are the constraint conditions, where Eq. (2) is an equality constraint, Eq. (3) is an inequality constraint, and Eq. (4) is a parameter constraint. For standard ACOPF, the to-be-optimized vector x includes voltage angles Θ, voltage magnitudes V_m, generator real power output and reactive power output P_g and Q_g, where the voltage phase angle and voltage magnitudes are the vector of $n_b \times 1$ (n_b represents the number of buses or nodes in the grids), and the real power and reactive power are the vector of $n_g \times 1$ (n_g represents the number of generators or power supplies in the grid).

$$x = \begin{bmatrix} \Theta \\ V_m \\ P_g \\ Q_g \end{bmatrix} \tag{5}$$

For each generator, objective function (1) is summation of individual polynomial cost functions f_P^i and f_Q^i of real and reactive power injections:

$$\min_{\Theta, V_m, P_g, Q_g} \sum_{i=1}^{n_g} f_P^i(p_g^i) + f_Q^i(q_g^i) \tag{6}$$

Equality constraint in (2) can be divided into real power balance constraint and reactive power balance constraint as below:

$$g_P(\Theta, V_m, P_g) = P_{bus}(\Theta, V_m) + P_d - C_g P_g = 0 \tag{7}$$
$$g_Q(\Theta, V_m, Q_g) = Q_{bus}(\Theta, V_m) + Q_d - C_g Q_g = 0 \tag{8}$$

Inequality constraint (3) consist of two sets of n_l branch flow limits as nonlinear functions of the bus voltage angles and magnitudes, one for the *from* end and one for the *to* end of each branch:

$$h_f(\Theta, V_m) = \left|F_f(\Theta, V_m)\right| - F_{\max} \le 0 \tag{9}$$
$$h_t(\Theta, V_m) = |F_t(\Theta, V_m)| - F_{\max} \le 0 \tag{10}$$

Where F_{max} is the vector of flow limits of the branch. The flows are typically apparent power flows expressed in MVA, but can be real power or current flows, yielding the following three possible forms for the flow constraints:

$$F_f(\Theta, V_m) = \begin{cases} S_f(\Theta, V_m) \\ P_f(\Theta, V_m) \\ I_f(\Theta, V_m) \end{cases} \tag{11}$$

Where S_f, P_f and I_f respectively refer to apparent power, real power and current. And S_f is calculated by using the following equation:

$$S_f(V) \quad = [C_f V] I_f^* = [C_f V] Y_f^* V^* \tag{12}$$

while I_f can be calculated by using the admittance matrix Y_f,

$$I_f = Y_f V \tag{13}$$

where Y_f is the admittance matrix of $n_l \times n_b$, and n_l is the number of branches.

Parameter constraints in Eq. (4) include: reference node voltage phase angle constraint, node voltage upper and lower limits, generator real power injection and reactive power injection limits. Details are as follows:

$$\theta_i^{\text{ref}} \le \theta_i \le \theta_i^{\text{ref}}, \qquad i \in \Gamma_{\text{ref}} \tag{14}$$
$$v_m^{i,\min} \le v_m^i \le v_m^{i,\max}, \qquad i = 1, 2, \ldots, n_b \tag{15}$$
$$p_g^{i,\min} \le p_g^i \le p_g^{i,\max}, \qquad i = 1, 2, \ldots, n_g \tag{16}$$
$$q_g^{i,\min} \le q_g^i \le q_g^{i,\max}, \qquad i = 1, 2, \ldots, n_g \tag{17}$$

S7. Check if ACOPF converges. If the calculated result converges, then the result is saved. If not, it is very likely that the system load itself cannot meet the requirement. At this point of time, part of system load is removed in order to meet the load needs of most system nodes.

S8. Conduct an ACPF (Alternating Current Power Flow) analysis of the said island [25], in order to obtain load of all branches and identify the overloaded branches.

S9. Identify the branch having the highest percentage of overload based on the ACPF calculation result; and then find out all loads within the radius R of that connecting line. Conduct a load shedding treatment of these nodes by making a reference to Manchester model. Shed 5% of the load of each node, and then use ACOPF to check if convergence happens.

S10. Repeat the steps described in S9 to see if ACOPF converges within 20 load shedding. If convergence can be achieved, then the result shall be saved.

S11. If convergence can still not be achieved after 20 load shedding, then the branch with the highest overload shall be removed. Removal of the said branch may cause the power grids to split into more isolated islands. Therefore, the steps described in S1 through S10 shall be repeated until all island cascading failures stop and no more branches would become overloaded any more.

3. Case studies

Herein ACCF model is studied by taking IEEE 30 and 118-bus systems as examples. IEEE 30 and 118-bus systems are the test systems widely used in today's scientific research. Prototype of these test systems is part of the power grids in the United

States. We have extracted relevant data of IEEE 30 and 118-bus systems from the source code package of MATPOWER v5.1 MATLAB [24]. Table 1 is a summary of the parameters relevant to the IEEE 30 and 118-bus systems. The IEEE 30-bus system contains six power supply nodes, 24 substation nodes, 20 load nodes and 41 branches, where the load nodes can either be substation nodes or power supply nodes. The IEEE 118-bus system contains 54 power supply nodes, 64 substation nodes, 99 load nodes and 186 branches.

4. Results and discussion

Let us take IEEE 30-bus system as an example and assume the initial failures are Nodes n_1, n_2 and n_3. Fig. 1 demonstrates the cascading failure diffusion process.

The simulation results indicate that after Nodes n_1, n_2 and n_3 fail, Branches $l_1 - l_6$ lose connection along with the nodes (red dotted branches in Fig. 1(b)). Re-distribution occurs to the power flow of the grids and overload phenomenon occurs to Branches l_{11}, l_{22}, l_{29} and l_{32} (pink solid branches in Fig. 1(b)).

Subsequently, the model removes, in a certain proportion, the loads near the branch (l_{22}) with the highest overload rate (pink nodes in Fig. 1(c)).

However, even though part of the loads have been removed, steady state can still not be achieved for the grid, and some branches are still in an overloaded state. At this point, the branch with highest overload rate will become faulty according to the model setup, and thus, l_{22} becomes faulty and be removed, as shown in Fig. 1(d).

Redistribution of the power flow of the grids follows, which has resulted in overload of other branches, and then load shedding recurs, however, the power flow distribution is still unstable, and the branch l_{32} with the highest overload rate becomes faulty, as shown in Fig. 1(e).

The grids cascading failure continues to spread, and Branches l_{21}, l_{33}, l_{28}, l_{37}, l_{30} and l_{40} break up one after another, and the power grids splits into eight isolated islands and becomes stable at last. Each island is represented by one of the green shadow areas in Fig. 1(f). The eight islands respectively include 1, 1, 1, 1, 1, 3, 4 and 18 nodes as well as 0, 0, 0, 0, 0, 3, 3 and 21 branches.

We have noticed that Branches $l_7 - l_{10}$, which are the closest to the initial failure, have not broken up, while branches further away from the initial failure nodes have broken up in this cascading failure, such as l_{37} and l_{40}. In fact, in a cascading failure actually, broken branches are not necessarily close to the initially faulty elements, sometimes, a cascading failure may occur hundreds of kilometers away from the initial failure nodes/branches. This has been proven in a number of publications [26].

The foregoing has been a severe cascading failure process. The initially removed three nodes contain two power supplies (Nodes n_1 and n_2), and both of them have a fairly high power supply, which has resulted in power supply strain of the power grid, and further caused severe cascading failure. And as a result, the cascading failure shown in Fig. 1 is a severe example. In fact, removal of other connecting branches or nodes of the same quantity may not result in such severe cascading failure in most cases.

In the following, we will discuss the distribution pattern of losses resulted from grids cascading failure after removing a certain quantity of nodes or branches.

We have calculated the probability density function (PDF) and cumulative distribution function (CDF) of the system real power loss percentage under different number of initial faulty nodes (FN).

Fig. 2 shows the PDF and CDF of real power loss proportion of the system under different number of initial faulty nodes of the IEEE 30-bus system, wherein the number of initial faulty nodes FN ranges from one to six. It is observed that, as the number of initial faulty nodes increases, the system real power loss probability function changes from "high and thin" to "short and fat", the system real power loss expectation increases gradually, and the maximum likelihood estimate (MLE) of real power loss also increases gradually.

Besides node failure, this paper also gives system real power loss probability distribution under different number of faulty branches (FL), as shown in Fig. 3. It can be seen that compared with the same number of faulty nodes, the real power loss caused by faulty connecting branches is comparatively small. We classify the loss into four different degrees: No loss, a certain loss, large loss and total system failure. It can also be seen that when FL is between one and six, the probability for no real power loss of the system is high; and there is a certain probability of a certain loss; the probability of large real power loss or total system failure is in fact not high.

Discussed above is the distribution of system real power loss under given number of initial faulty nodes or connecting branches. Considering that in real life the occurrence of failure always involves a certain probability regardless of nodes or connecting branches, we first assume that the nodes and/or connecting branches fail according to a certain probability, and use Monte Carlo Simulation [27] to simulate failure of the nodes and/or connecting branches. Subsequently we use ACCF model to simulate the grids cascading failure process, and finally come up with a summary of system real power loss probability density function (PDF) and cumulative distribution function (CDF) under different failure probabilities.

Fig. 4 shows the probability density function and cumulative distribution function of real power loss percentage of the IEEE 118-bus system under different initial node failure probabilities (p_b respectively being 0.01, 0.05, 0.1, 0.2 and 0.3). It can be seen that the real power loss is basically consistent with the normal distribution function except under extremely low failure probability. Of course, the higher the failure probability, the bigger the real power loss expectation and the bigger

Table 1
Parameters of IEEE 30 and 118-bus systems.

System	Category	No.	Real power (MW)			Reactive power (MVAr)			Rated power (MVA)		
			Total power	Min. power	Max power	Total power	Min. power	Max power	Total power	Min. power	Max power
IEEE 30	Generators	6	335	30	80	405.9	−20	150	–	–	–
	Loads	20	189.2	2.2	30	107.2	0.7	30	–	–	–
	Branches	41	–	–	–	–	–	–	1954	16	130
IEEE 118	Generators	54	9966.2	100	805.2	11777	−1000	1000	–	–	–
	Loads	99	4242	2	277	1438	0	113	–	–	–
	Branches	186	–	–	–	–	–	–	43148	16	4000

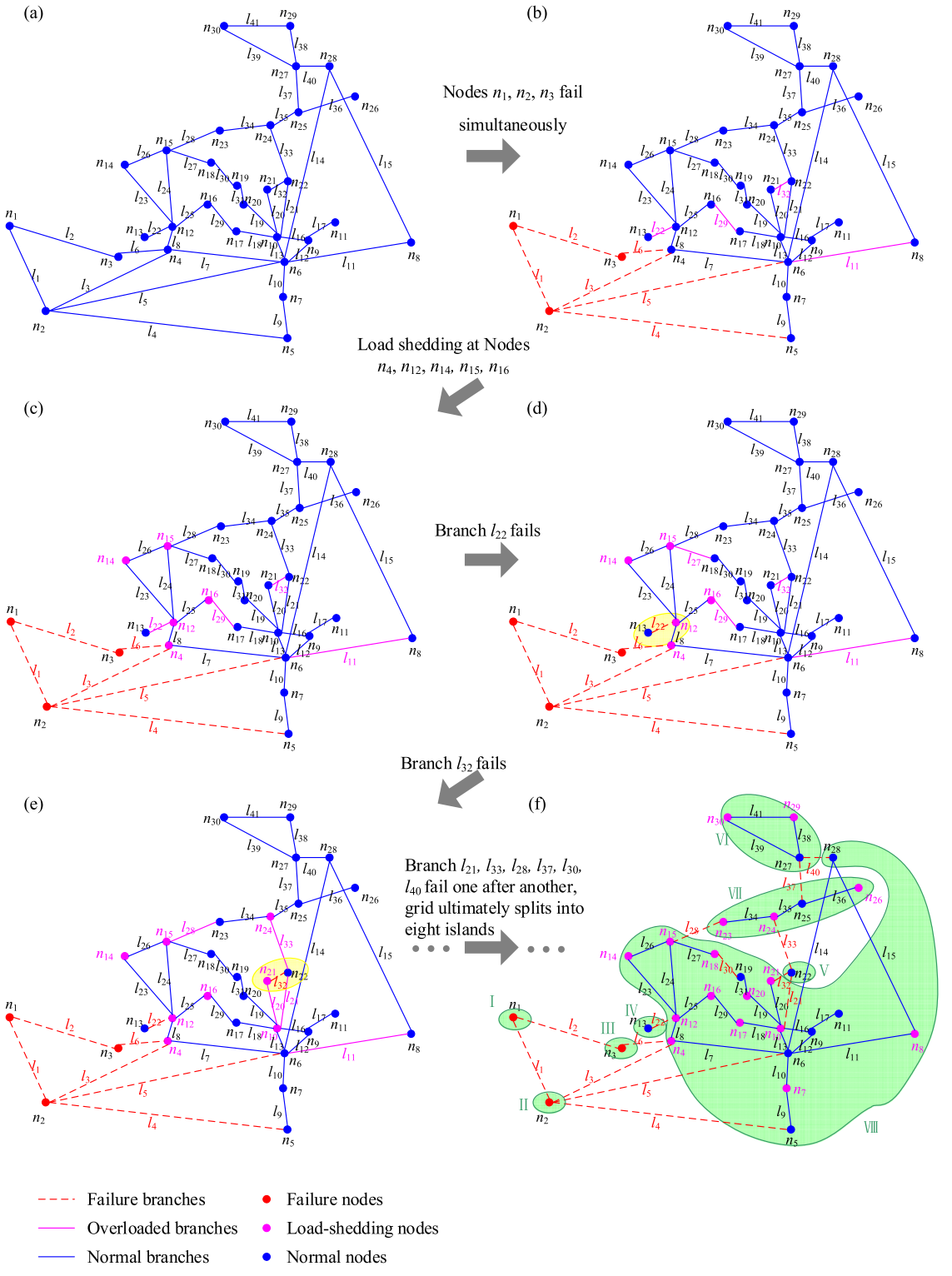

Fig. 1. Cascading failure process of IEEE 30-bus system (Nodes n_1, n_2, n_3 fail initially; Red dotted lines represent failed branches; pink solid lines represent overloaded branches; blue solid lines represent normally running branches; and pink nodes are load-shedding nodes). (For interpretation of the references to colour in this figure legend, the reader is referred to the web version of this article.)

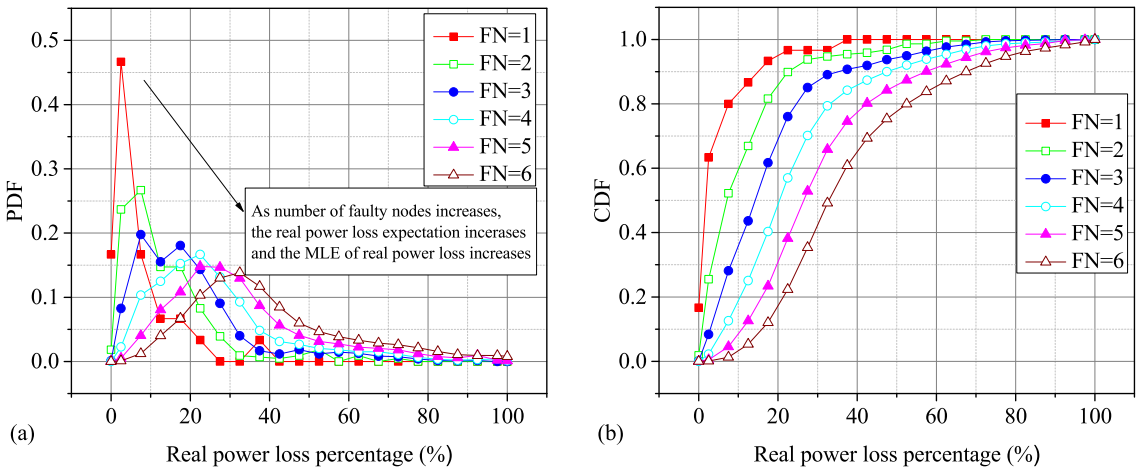

Fig. 2. Probability density function and cumulative distribution function of the system real power loss percentage under different number of initial faulty nodes: (a) PDF of real power loss percentage; (b) CDF of real power loss percentage.

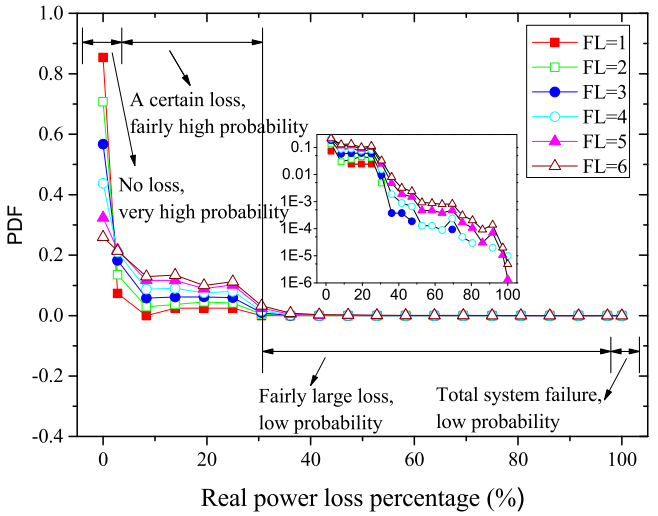

Fig. 3. Probability density function of real power loss percentage under different number of initial branch failure.

the maximum likelihood estimate (MLE) of real power loss. This is similar to the system loss distribution under different number of faulty nodes described above.

Fig. 5 shows the probability density function and cumulative distribution function of real power loss percentage of the IEEE 118-bus system under different initial branch failure probabilities (p_{br} respectively being 0.01, 0.05, 0.1, 0.2 and 0.3). As can be seen from the figure, after the connecting branches and nodes fail, characteristics of the system real power loss probability functions are in fact not the same. When the branch failure probability is small (for example, $p_{br} \leq 0.1$), the system real power loss approximately matches the power function, but when the failure probability is big (for example, $p_{br} \geq 0.3$), the system real power loss approximately matches a normal distribution function.

To investigate this phenomenon, we have simulated more operating conditions of the IEEE 30-bus system. In the simulation, the branch failure probability p_{br} respectively takes low failure probability (0.01 and 0.05), high failure probability (0.3 and 0.4) and extremely high failure probability (0.9 and 0.95). Histograms showing system real power loss distribution under different failure probabilities are given in Fig. 6. It can be seen that similar to the IEEE 118-bus system discussed above, when the branch failure probability is low, the system loss function approximately match the power function distribution. As the branch failure probability increases, the system loss gradually becomes a normal distribution function. When the branch failure probability further increases, the system loss distribution is approximately symmetric with 50% loss under low failure probability.

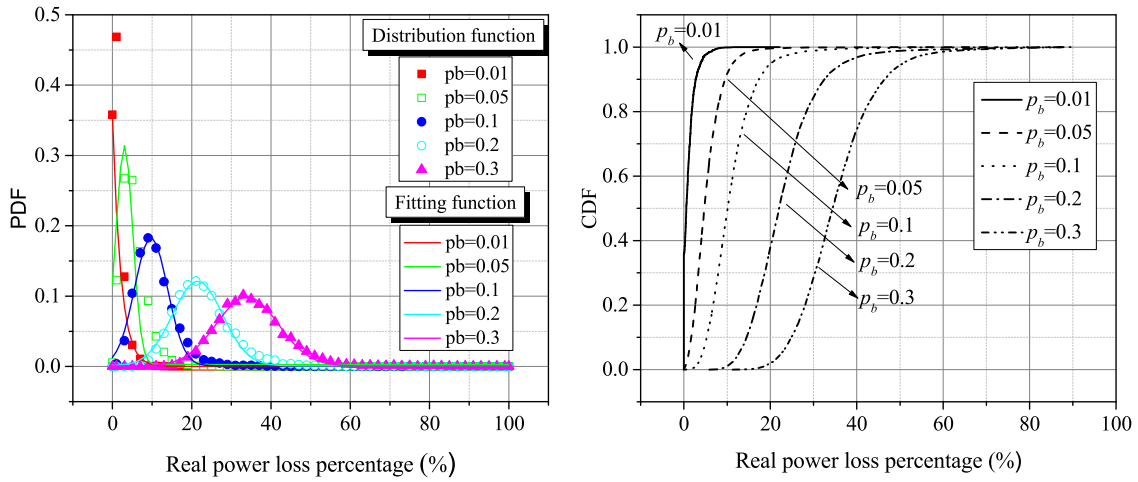

Fig. 4. System real power loss percentage under different probability of initial node failure: (a) Probability density function (PDF), curves being fitting result of probability function; (b) Cumulative distribution function (CDF).

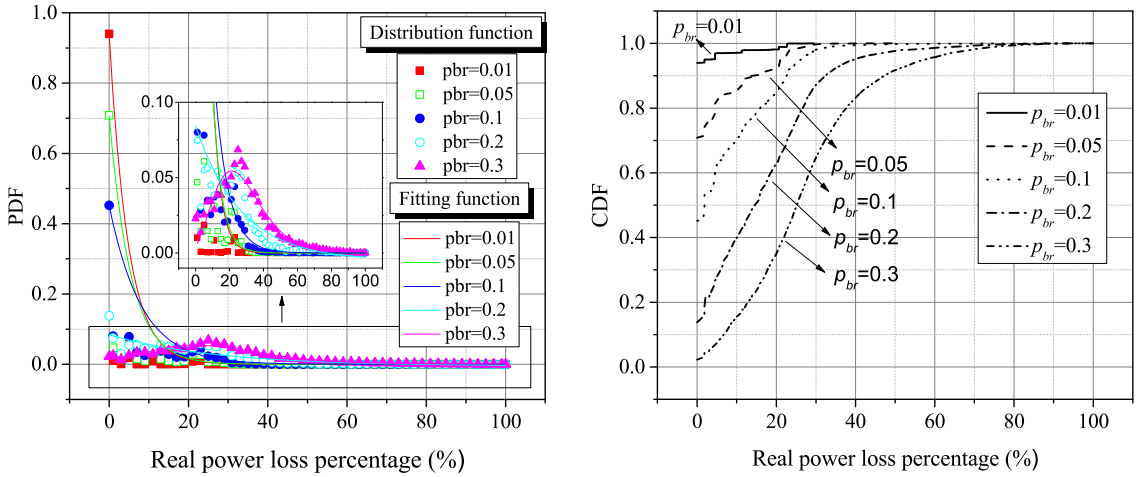

Fig. 5. System real power loss percentage under different initial failure probability of connecting branches: (1) Probability density function (PDF), curves being the fitting results of probability function; (2) Cumulative distribution function (CDF).

5. Conclusions

Major blackout accidents are usually caused by grids cascading failures. Furthermore, Grids cascading failure may also aggravate grids damage subsequent to natural disasters. Therefore, the prevention of cascading failure is a measure of great significance not only for ensuring grids safety and stable operation, but also for grids disaster prevention and relief. Simulating the grids cascading failure process is an essential means of preventing cascading failures.

Based on an AC-based Cascading Failure model (ACCF model), this paper introduces a non-linear optimization method to help speed up computation and avoid unconvergence. The model simulate the power flow status of each isolated island in the power grids, and when necessary, generator tripping and load shedding measures are taken to make sure that the grids could enter a steady state as fast as possible.

The ACCF model is applied to IEEE 30 and IEEE 118-bus system. The simulation indicates that this model can reflect the process in which the branches gradually break up and the nodes gradually lose connections during grids cascading failure. Meanwhile, it is found in the case study that during the cascading failure, the broken branches are not necessarily close to the initial faulty elements, and that some of the affected nodes/branches are “far” away from the initial faulty nodes.

This paper has studied the system loss distribution pattern under different number of initial faulty nodes and branches, and has also investigated the system loss distribution pattern under different node and branch failure probabilities. It is indicated that as the initial node failure probability or the number of initial node/branches failures increases, the system real power loss probability function changes from “high and thin” to “short and fat”, the system real power loss expectation

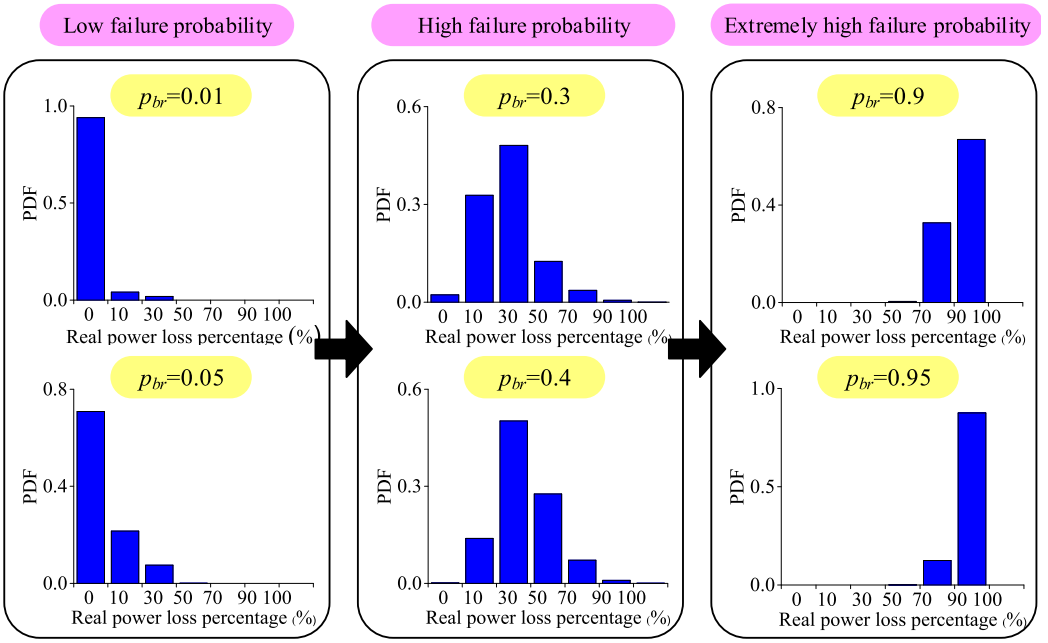

Fig. 6. Relationship between probability density distribution characteristics of real power loss percentage and branch failure probability (p_{br}).

gradually increases and the maximum likelihood estimate of real power loss also increases gradually. And as the initial branch failure probability increases, the system real power loss probability function gradually changes from approximate power distribution to normal distribution. Meanwhile, the study also discovers that as the initial branch failure probability further increases, the system real power loss changes from normal distribution to a distribution appearing to be symmetric with the loss function under a low initial branch failure probability.

The findings could facilitate grids safety and stable operation, as well as grids disaster prevention and relief. In this study, a representative cascading failure process is presented while it is assumed several nodes are failed initially. As an alternative, the cascading process could also be recorded by the ACCF model when the branches are assumed to be failed initially. It should also be noted that though the ACCF model captures AC power flow and optimal power flow, and considers economic dispatch, some of the grids characteristics are not taken into consideration, e.g. short-circuit propagation in a station or the entire grid, and the future research will emphasize this.

Acknowledgments

This study is financially supported by the National Key Research and Development Project of China through grant 2016YFC0802500, the National Natural Science Foundation of China (NSFC) through grants 51622403, 51576212, 51674152 and 71774148, Beijing Science and Technology Special Project through grant Z171100001117145, and the Basic Research Fund of China Academy of Safety Science and Technology, China through grants 2018JBKY02 and 2017JBKY03. This work is also funded in part by the U.S. Department of Defense, United States through the MURI grant W911NF-13-1-0340 and the U.S. National Science Foundation (NSF), United States through grant CMMI-1435845.

References

[1] V. Rampurkar, P. Pentayya, H.A. Mangalvedekar, et al., Cascading failure analysis for Indian power grid, IEEE Trans. Smart Grid 7 (4) (2016) 1951–1960.
[2] J. Bialek, E. Ciapessoni, D. Cirio, et al., Benchmarking and validation of cascading failure analysis tools, IEEE Trans. Power Syst. 31 (6) (2016) 4887–4900.
[3] Min Ouyang, Min Xu, Chi Zhang, et al., Mitigating electric power system vulnerability to worst-case spatially localized attacks, Reliab. Eng. Syst. Saf. 165 (2017) 144–154.
[4] J. Wang, L. Rong, L. Zhang, Z. Zhang, Attack vulnerability of scale-free networks due to cascading failures, Physica A 387 (26) (2008) 6671–6678.
[5] Z. Chen, W.B. Du, X.B. Cao, et al., Cascading failure of interdependent networks with different coupling preference under targeted attack, Chaos Solitons Fractals 80 (2015) 7–12.
[6] S.U.N. Yushu, T. Xisheng, Cascading failure analysis of power flow on wind power based on complex network theory, J. Mod. Power Syst. Clean Energy 2 (4) (2014) 411–421.
[7] J. Yan, Y. Tang, H. He, et al., Cascading failure analysis with DC power flow model and transient stability analysis, IEEE Trans. Power Syst. 30 (1) (2015) 285–297.
[8] G. Chen, X. Wang, X. Li, Fundamentals of Complex Networks: Models, Structures and Dynamics, John Wiley & Sons, 2014.

[9] A.E. Motter, Y. Lai, Cascade-based attacks on complex networks, Phys. Rev. E 66 (2002) 65102.
[10] G.A. Pagani, M. Aiello, The power grids as a complex network: A survey, Physica A 392 (11) (2013) 2688–2700.
[11] P. Crucitti, V. Latora, M. Marchiori, Model for cascading failures in complex networks, Phys. Rev. E 69 (4) (2004) 45104.
[12] Z. Chen, W.B. Du, X.B. Cao, et al., Cascading failure of interdependent networks with different coupling preference under targeted attack, Chaos Solitons Fractals 80 (2015) 7–12.
[13] Q. Chen, J.D. McCalley, A cluster distribution as a model for estimating high-order event probabilities in power systems, Probab. Engrg. Inform. Sci. 19 (4) (2005) 489–505.
[14] M. Ouyang, L. Dueñas-Osorio, Resilience modeling and simulation of smart grids, in: Structures Congress 2011, 2011, pp. 1996–2009.
[15] I. Dobson, Estimating the propagation and extent of cascading line outages from utility data with a branching process, IEEE Trans. Power Syst. 27 (4) (2012) 2146–2155.
[16] M. Manning, J.M. Carlson, J. Doyle, Highly optimized tolerance and power laws in dense and sparse resource regimes, Phys. Rev. E 72 (1) (2005) 016108.
[17] D. Marković, C. Gros, Power laws and self-organized criticality in theory and nature, Phys. Rep. 536 (2) (2014) 41–74.
[18] X. Liu, Z. Li, Revealing the impact of multiple solutions in DCOPF on the risk assessment of line cascading failure in OPA model, IEEE Trans. Power Syst. 31 (5) (2016) 4159–4160.
[19] J. Chen, J.S. Thorp, I. Dobson, Cascading dynamics and mitigation assessment in power system disturbances via a hidden failure model, Int. J. Electr. Power Energy Syst. 27 (4) (2005) 318–326.
[20] B.A. Carreras, V.E. Lynch, I. Dobson, et al., Critical points and transitions in an electric power transmission model for cascading failure blackouts, Chaos 12 (4) (2002) 985–994.
[21] R.D. Zimmerman, C.E. Murillo-Sanchez, R.J. Thomas, MATPOWER: Steady-state operations, planning, and analysis tools for power systems research and education, IEEE Trans. Power Syst. 26 (1) (2011) 12–19.
[22] J. Tomaney, A. McCarthy, The Manchester model, Town Ctry. Plan. 84 (5) (2015) 233–236.
[23] J. Li, L. Dueñas-Osorio, C. Chen, et al., AC power flow importance measures considering multi-element failures, Reliab. Eng. Syst. Saf. 160 (2017) 89–97.
[24] R.D. Zimmerman, C.E. Murillo-Sanchez, R.J. Thomas, MATPOWER: Steady-state operations, planning, and analysis tools for power systems research and education, IEEE Trans. Power Syst. 26 (1) (2011) 12–19.
[25] W.F. Tinney, C.E. Hart, Power flow solution by Newton's method, Power Appar. Syst. 11 (1967) 1449–1460.
[26] A. Bernstein, B. Daniel, H. David, et al., Power grids vulnerability to geographically correlated failures –analysis and control implications: IEEE INFOCOM 2014, in: IEEE Conference on Computer Communications, 2014.
[27] R.Y. Rubinstein, D.P. Kroese, Simulation and the Monte Carlo Method, John Wiley & Sons, 2016.